Effects of Foreground Augmentations in Synthetic Training Data on the Use of UAVs for Weed Detection

Simon Hallösta*[1], Mats I. Pettersson[1], and Mattias Dahl[1]

[1]Blekinge Institute of Technology
{simon.hallosta, mats.pettersson, mattias.dahl}@bth.se

Abstract

This study addresses the issue of black-grass, a herbicide-resistant weed that threatens wheat yields in Western Europe, through the use of high- resolution Unmanned Aerial Vehicles (UAVs) and synthetic data augmentation in precision agriculture. We mitigate challenges such as the need for large labeled datasets and environmental variability by employing synthetic data augmentations in training a Mask R-CNN model. Using a minimal dataset of 43 black-grass and 12 wheat field images, we achieved a 37% increase in Area Under the Curve (AUC) over the non-augmented baseline, with scaling as the most effective augmentation. The best model attained a recall of 53% at a precision of 64%, offering a promising approach for future precision agriculture applications.

1 Introduction

The agricultural industry globally grapples with various invasive weeds, of which black-grass (Alopecurus myosuroides) has emerged as the most problematic in Western Europe [1]. This weed's herbicide resistance and aggressive growth patterns significantly impact wheat yield, particularly when densities surpass 10 plants per m^2 [2].

To tackle this issue, precision agriculture, empowered by technologies such as Unmanned Aerial Vehicles (UAVs), offers promising avenues for enhancing agricultural productivity [3]. UAVs endowed with high-resolution imaging, provide rapid and efficient surveying of large crop fields [4].

However, integrating UAVs for weed detection is not without challenges. The demands for labeled data when training computer vision models and the problem of domain shift, owing to varying environmental and crop conditions, are substantial roadblocks [5]. In this context, synthetic data offers a compelling solution. It not only alleviates the need for manual data labeling but also addresses data variability issues [6]. Furthermore, targeted synthetic data augmentation can significantly improve model generalization across datasets [6].

This study investigates the impact of synthetic data augmentations on deep-learning models tailored for black-grass detection in wheat fields. We focus on identifying which augmentation combinations are most effective and how they can reduce training time. This knowledge is crucial for quickly adapting models to the variable conditions often observed across different fields.

1.1 Related works

The area of weed detection in agricultural fields using Unmanned Aerial Vehicles (UAV) and machine learning has been an active research field, with various methodologies being proposed. A popular approach is using Convolutional Neural Networks (CNNs) as primary tools for detection and classification, such as in the study by Valente et al. [7] where AlexNet was used for detecting weed in grassland.

Deep learning models have been broadly applied, with Bah et al. [4] proposing a deep learning approach with unsupervised data labeling for weed detection, achieving performance comparable to supervised learning methods. Similarly, Etienne et al. [8] utilized a YOLOv3 network for detecting weeds in soybean and corn fields, while Wang et al. [9] presented a TIA-YOLOv5 network, both achieving high precision rates.

Another deep learning model that has been used is the Mask R-CNN. Milioto et al. [10] applied it for real-time weed detection in sugar beet fields. Similarly, Valicharla et al. [11] used a pre-trained Mask R-CNN with ResNet-50 FPN for invasive weed detection.

However, more approaches have been proposed where multiple techniques have been combined into a final model. The work by Mu et al. [12] incorporated a feature pyramid network (FPN) algorithm into a Faster R-CNN network for enhanced recognition accuracy. A combination of Houghlines and Random Forest also proved to be effective, as evidenced by Gao et al. [13]. El-kenawy et al. [14] proposed a voting classifier with base models consisting of neural networks, support vector machines, and K-nearest neighbors.

The topic of synthetic training data has also been explored, with Hu et al. [15] showing that semi-supervised learning boosted weed detection when

*Corresponding Author.

Proceedings of the 5th Northern Lights Deep Learning Conference (NLDL), PMLR 233, 2024.

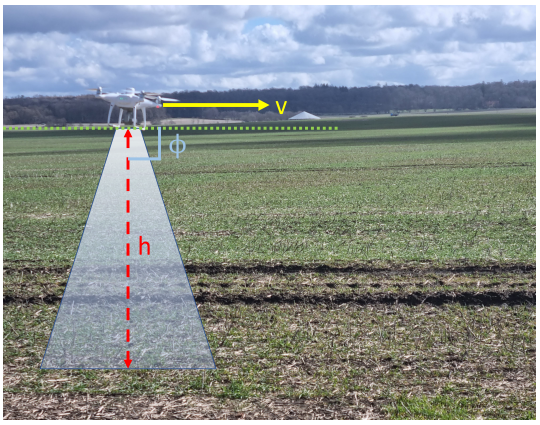

Figure 1. The UAV collecting data in a wheat field at the height h, velocity v and with a camera angle, Φ, perpendicular to the ground.

combined with synthetic data. Xie et al. [16] used a skeleton annotation approach for foreground uncertainty in labeling, along with synthetic data. This is closely related to Sapkota et al. [17], who used synthetic images, generated using GANs and data augmentations, to improve weed detection.

Notably, several works have focused on black-grass detection in particular, an area of interest in our work. Su et al. [18] have experimented with multispectral imaging for black grass detection, and Lambert et al. [19] employed semantic segmentation in wheat fields. The investigation of synthetic images, data augmentations, and Mask R-CNN in these works forms a pertinent context for our research.

2 Method

In this section, we describe our approach for weed detection and identification using synthetic data and deep learning. We cover the data collection, preprocessing, data augmentation, deep learning model, evaluation metrics, and experimental setup.

2.1 Data Collection

Data were acquired using a UAV fitted with a high-definition RGB camera, flying over farmland in southern Sweden. Additional video was captured in non-infested fields to collect background data for synthetic data generation, see section 2.2.

The UAV operated at altitudes between [0.5-1.5] m above ground, at speeds between [0.3-1.0] m/s, minimizing motion blur, Fig 1. To optimize object coverage, the camera was aligned at the nadir point and rotated 90° relative to the flight direction. This optimized the 16:9 aspect ratio camera's field of view, enabling prolonged object retention within the frame.

Video data were captured at 60 frames per second (FPS) with a 2.7k resolution, maximizing detail for effective weed identification. Alongside the UAV footage, high-resolution stationary photos of black-grass were taken using cell phones, broadening the range of black-grass appearances in our dataset. These photos, together with the video frames, underwent pixel-level extraction of black-grass instances, forming a comprehensive foreground dataset.

The test data was collected from the same field on a single day, maintaining consistent conditions, while parts of this field were also used for gathering background and foreground data for synthetic data creation. This approach mirrors potential real-world applications of our method, ensuring relevance and applicability.

2.2 Synthetic Data Generation and Augmentations

For synthetic data generation, we select a random background image I_{bg_j} from the set B, and a random subset F_{fg} from the set F of all foreground images.

$$
\begin{aligned}
\text{Scaling:} \quad & I_{\text{fg}_i}^{\{s\}} = \text{S}(I_{\text{fg}_i}, 1+s), && s \sim \text{U}(-0.25, 0.25) \\
\text{Rotation:} \quad & I_{\text{fg}_i}^{\{r\}} = \text{R}(I_{\text{fg}_i}, \theta), && \theta \sim \text{U}(-180, 180) \\
\text{Mirroring:} \quad & I_{\text{fg}_i}^{\{m\}} = \text{M}(I_{\text{fg}_i}, m), && m \sim \text{Bern}(0.5) \\
\text{Brightness:} \quad & I_{\text{fg}_i}^{\{b\}} = \text{B}(I_{\text{fg}_i}, \phi), && \phi \sim \text{U}(0.8, 1.2).
\end{aligned}
$$

By implementing selected augmentations on the foreground and then overlaying it onto the background, a new synthetic image paired with ground truth is generated. Corresponding masks are synthesized based on the foreground's locations within this composite image, see Figure 2.

We introduce $S^{\{*\}}$ to represent the power set of all combinations of the four transformations. This yields $\sum_{k=0}^{4} \binom{4}{k} = 16$ distinct subsets. Each subset, such as $S^{\{s,r\}} \subset S^{\{*\}}$, indicates a specific combination of augmentations, in this case, scaling (s) and rotation (r). By iterating over all subsets of $S^{\{*\}}$, we generate multiple synthetic datasets, each reflecting a distinct set of augmentations. Specifically, from an initial set of 43 foreground images featuring black-grass and 12 background images of wheat fields without black-grass occurrences, we produced a total of 1000 synthetic training examples for each augmentation set $S^{\{*\}}$.

2.3 Model Selection

The Mask R-CNN architecture equipped with a ResNet-50 FPN pre-trained on the MSCOCO dataset was chosen for our experiments [20]. This decision is grounded in a broad scholarly consensus, highlighting Mask R-CNN's effectiveness in a variety of object detection tasks [10, 11, 15, 16, 20].

(a) Synthetic image

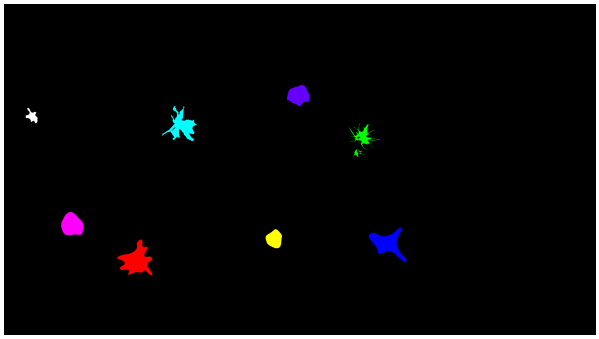

(b) Ground truth mask

Figure 2. Example of synthetic data used in training. (a) shows the synthetic image, and (b) the corresponding generated ground truth masks.

A study by Valicharla et al. [11] particularly emphasized the suitability of ResNet-50 for weed species detection. While larger backbones like ResNet-101 have been reported to yield marginal performance gains [20], we favored ResNet-50 for its balance between performance, computational efficiency, and model complexity. Resource constraints and the volume of training were pivotal factors in this choice.

2.4 Model Training

Each dataset in $S^{\{*\}}$ was used to train an independent Mask R-CNN model with a ResNet-50 FPN backbone, which had been pre-trained on MSCOCO. Our training protocol is designed in a two-phased manner to evaluate the synthetic data augmentations' effectiveness.

In the first phase, we train the head of the Mask R-CNN for four epochs with the Adam optimizer. For the second phase, we fine-tune the entire network for another four epochs, but at a learning rate of one-tenth of that used in the initial phase. We decrease the learning rate to mitigate catastrophic learning.

This eight-epoch training scheme was deliberately chosen, aligning with the practical requirements of rapid adaptability to fluctuating field conditions. By doing so, we achieve a compromise between comprehensive training and real-world applicability, making the method apt for immediate field deployments.

2.5 Model Evaluation

We employed various metrics to assess model efficacy in detecting Black Grass. The primary metric was Intersection over Union (IoU):

$$\text{IoU} = \frac{|A_P \cap B_{GT}|}{|A_P \cup B_{GT}|}$$

Here, A_P and B_{GT} denote predicted and ground truth regions. Additional metrics included precision (P), recall (R), and the f1-score:

$$f_1 = \frac{2 \cdot P \cdot R}{P + R}$$

Lastly, the Area Under the Curve (AUC) of the Precision-Recall curve served as a holistic metric, summarizing the trade-off between P and R at various threshold levels.

2.6 Test Data

To evaluate model performance, we sourced test data from a drone video surveying a field infected with Black Grass. Frames were selectively captured from the video, and each was manually annotated to mark instances of Black Grass, serving as the ground truth for model evaluation.

Annotations relied solely on visual cues within the frames, excluding any contextual or supplementary information from the data collection phase. This limitation in the annotation process necessitated a refined evaluation strategy.

To address this, we designed a grading system that encompasses varying levels of difficulty in visually identifying Black Grass instances. Bounding boxes were scored on a 0-4 scale (*Easiest, Easy, Medium, Hard, Hardest*), gauging the complexity of visual detection. The graded dataset consist of 653 instances distributed as 102 *Easiest*, 120 as *Easy*, 165 as *Medium*, 132 as *Hard*, and 134 as *Hardest*.

Grades were determined using traits such as weed size, effective resolution influenced by factors like motion blur and lighting, separation from other plants, turf density indicating tangled complexity, and occlusion by other structures. Grading decisions were made based on the first category where all criteria were met, as detailed in Table 1. Examples of graded plants can be found in Fig 3.

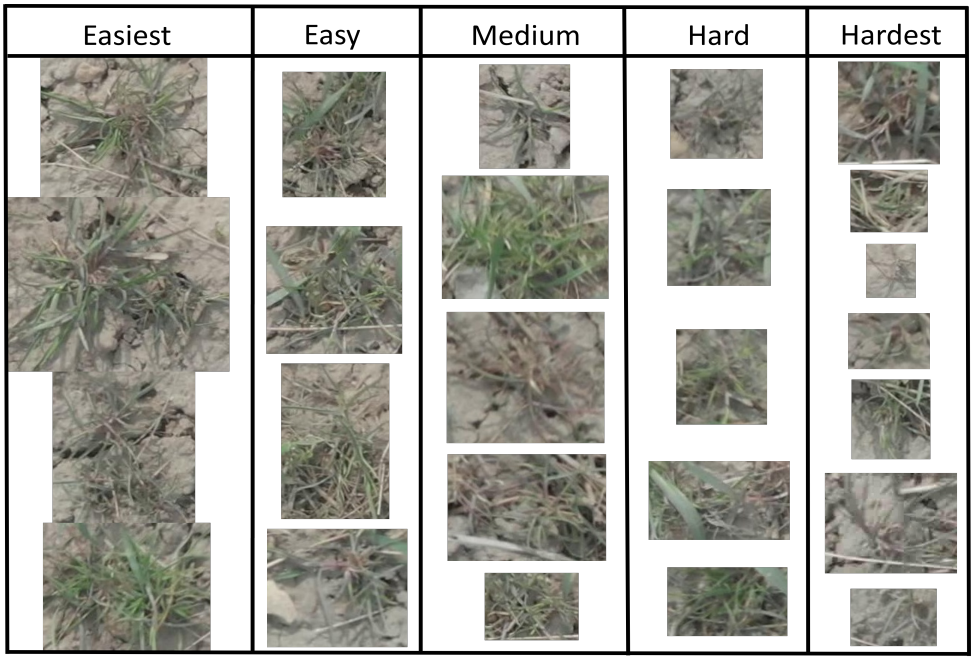

Figure 3. Instances of Black Grass plants in the graded test dataset. Each column corresponds to examples of grades Easiest to Hardest (grades 0 through 4). Adhering to the grading procedure described in Table 1.

Table 1. Grades for each black grass instance in the test set are determined by the first category, in descending difficulty, where all criteria are met.

Trait	Grades				
	Easiest	***Easy***	***Medium***	***Hard***	***Hardest***
Weed Size	Large	Large-Medium	Medium-Small	Medium-Small	Small
Resolution	Excellent	Good	Good-Low	Low	Low
Separation	Yes	Yes	No	No	No
Structure	Dense	Dense	Moderate	Sparse	Very sparse
Occlusion	No	No	No	Yes	Yes

3 Results

This section evaluates the performance of Mask R-CNN models, each trained on a distinct synthetic dataset with a ResNet-50 FPN backbone pretrained on MSCOCO, for parameter consistency.

3.1 Combined grades

We assessed the impact of augmentations on model performance through various metrics. The Precision-Recall-curve without grading considerations reveals that the *Scale* model excelled, achieving the highest AUC (0.52) and maintaining high precision at a recall beyond 0.37 (Figure 4). Among others, *Brightness Rotate* ranked second in AUC (0.46), while *No Augmentation* occupied a mid-range AUC (0.39).

Table 2. Metrics for all models on the test dataset, ignoring black grass difficulty grades. The control model, $S^{\{\emptyset\}}$, had no augmentations. Sorted by F1-score, predictions are accepted at a prediction score above 0.4 and count as positive identification at an IoU of 0.25.

Augmentations	Recall	Precision	f1
$S^{\{s\}}$	**0.53**	0.64	**0.58**
$S^{\{b,r\}}$	0.47	0.63	0.54
$S^{\{s,r\}}$	0.45	0.63	0.52
$S^{\{s,b,m\}}$	0.40	0.68	0.50
$S^{\{m\}}$	0.40	0.69	0.50
$S^{\{s,b\}}$	0.38	0.72	0.50
$S^{\{\emptyset\}}$	0.46	0.54	0.50
$S^{\{s,m\}}$	0.39	0.67	0.50
$S^{\{b,r,m\}}$	0.39	0.62	0.48
$S^{\{s,b,r,m\}}$	0.38	0.61	0.47
$S^{\{r\}}$	0.37	0.63	0.47
$S^{\{s,b,r\}}$	0.34	0.71	0.46
$S^{\{s,r,m\}}$	0.33	0.77	0.46
$S^{\{b\}}$	0.33	0.73	0.46
$S^{\{r,m\}}$	0.27	0.79	0.41
$S^{\{b,m\}}$	0.25	**0.89**	0.40

The AUC metric fails to fully capture models excelling in precision but lacking in recall. For instance, *No Augmentation* showed weak precision across recall ranges despite its decent AUC.

In Table 2, we note a pattern consistent with Figure 4. The *Scale* model led in f1-score, followed by *Brightness Rotate*, with *No Augmentation* holding a middle rank.

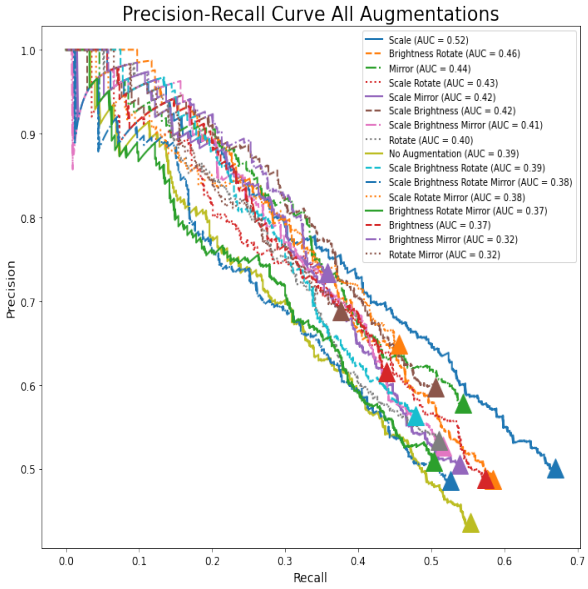

Figure 4. Precision-Recall curve for all models trained on the different augmentation combinations. These are the combined results when not accounting for the grades in the test set. The legend is ordered from highest AUC to lowest.

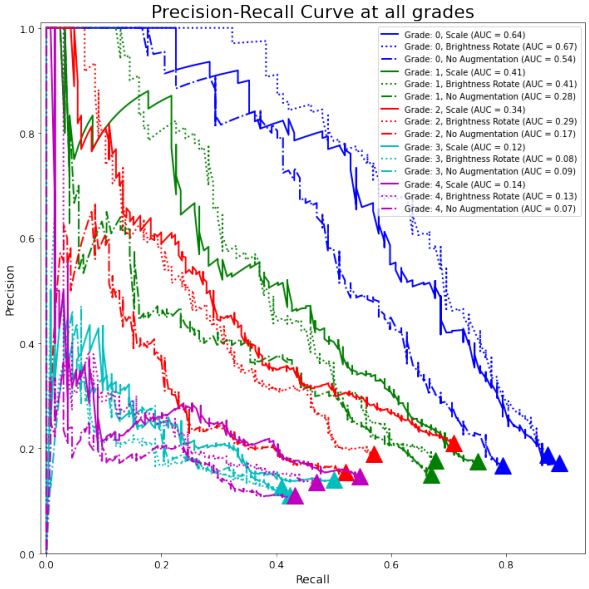

Figure 5. Precision-Recall curve of the models trained with the augmentations: Scale, Brightness and Rotation, and No Augmentations. The different colors indicate the grade and the line style the model. Grades are coloured according to: 0-Blue, 1-Green, 2-Red, 3-Teal, 4-Purple.

3.2 Graded test data

We gauged model performance on graded test data, focusing on both easier (grades 0, 1) and harder instances (grades 3, 4) using f1-score. Counterintuitively, high-performing models on difficult instances did not always excel on easier ones, as Table 3 indicates. The *Scale* model, for instance, was adept at identifying harder examples but suffered lower precision on easier ones.

On comparing *Scale*, *Brightness Rotate*, and *No Augmentation*, the former two closely matched for grades 0 and 1. However, *Scale* outperformed in grades 2-4, while the control lagged behind (Figure 5).

4 Discussion

Detecting invasive species like black-grass presents a challenge due to the limited availability of real-world data. In this study, we mitigated this issue by utilizing synthetic data augmented with various transformations. Our analysis illuminates the impact of these augmentations and explores the constraining role of limited training time on model performance.

Among the augmentations applied, scaling was particularly impactful. It yielded the best results in terms of recall, f1-score, and AUC on the PR-curve, as evidenced by Table 2 and Figure 4. On the non-graded dataset it had an 37% increase in AUC over the baseline model. Since results were achieved with a small dataset and only using synthetic data it could be applied in fine-tuning the model to the specific field condition.

Data augmentations are known to improve model generalization [4, 9, 15]. However, our limited training time of 8 epochs necessitates caution in selecting augmentations, as more complex methods could impede effective learning.

A comparison of our best models with a non-augmented baseline, Figure 5, shows significant gains in AUC and average f1-score, particularly for the Scale model in complex black-grass instances. Scaling encompasses a wide range of sizes, from small and occluded to larger instances, providing a more realistic training environment. This diversity is crucial for accurately detecting our test sets' typically

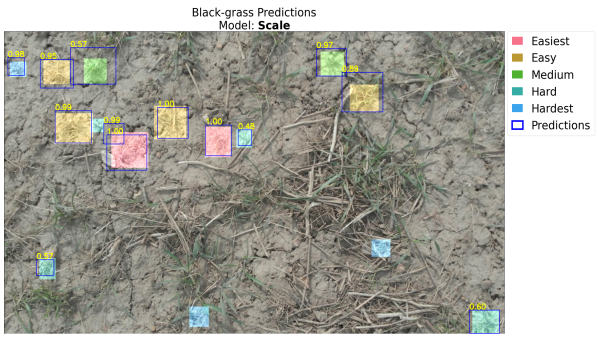

Figure 6. Predictions from the *Scale* model with varied color gradings to represent difficulty. The model successfully identified all black grass labeled as *easiest*, *easy*, and *medium* but failed to detect one *hard* and two *hardest* instances.

Table 3. Heat map table of f1-scores for all models on the graded test dataset. The table is sorted based on performance on grade 4, the hardest dataset. The models had a threshold of 0.4 in prediction score to accept proposed objects and an IoU of 0.25.

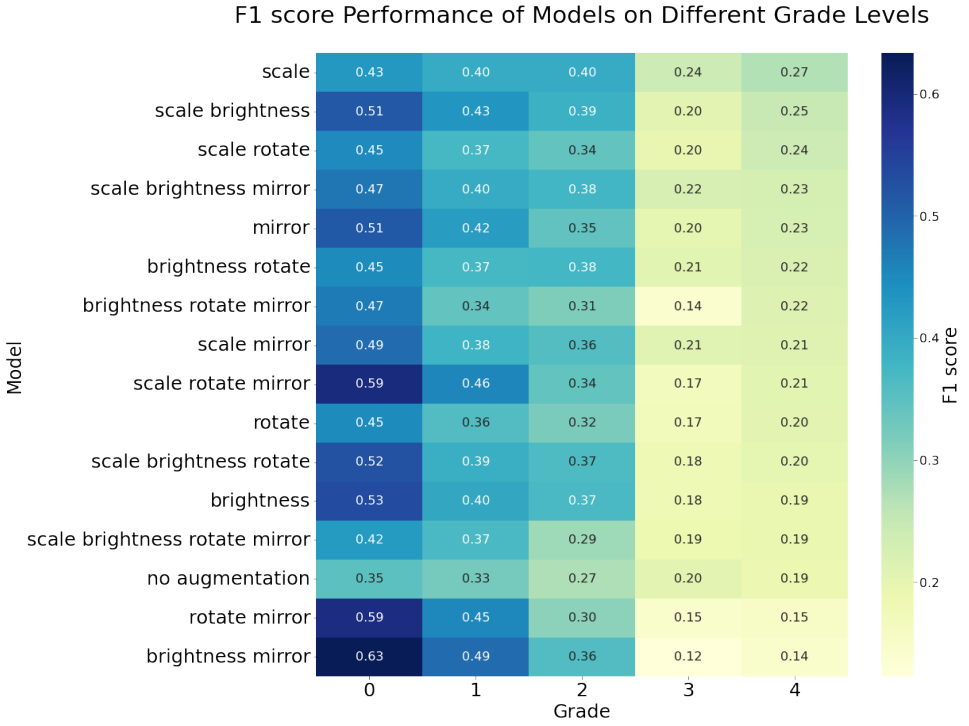

small and low-resolution hard samples. It introduces a balanced variety of instance sizes, facilitating more efficient model fine-tuning without adding excessive complexity to the data, thereby improving detection in real-world scenarios.

Future work could explore the interplay between augmentation complexity, training duration, and performance. Extended training or employing advanced training methods could further optimize the models for real-world application.

5 Conclusion

This study highlights the efficacy of data augmentation in black-grass detection using limited resources. With high- resolution UAV data, the 'Scale' model achieved a 37% increase in performance on the AUC metric compared to the non-augmented baseline. Employing a Mask R-CNN with a pre-trained ResNet-50 FPN, we attained 53% recall at 64% precision using only 43 black-grass and 12 wheat field images.

The results demonstrate the power of data augmentation for quick, resource-efficient adaptation to new detection challenges, critical for timely weed management in diverse fields.

References

[1] S. R. Moss, S. A. M. Perryman, and L. V. Tatnell. "Managing Herbicide-resistant Blackgrass (Alopecurus myosuroides): Theory and Practice". In: *Weed Technology* 21.2 (2007), pp. 300–309. DOI: 10.1614/WT-06-087.1.

[2] H. Mennan and D. Işik. "The Competitive Ability of Avena spp. and Alopecurus myosuroides Huds. Influenced by Different Wheat (Triticum aestivum) Cultivars". en. In: ().

[3] R. Gebbers and V. I. Adamchuk. "Precision Agriculture and Food Security". In: *Science* 327.5967 (Feb. 2010). Publisher: American Association for the Advancement of Science, pp. 828–831. DOI: 10.1126/science.1183899. URL: https://www.science.org/doi/10.1126/science.1183899 (visited on 06/20/2023).

[4] M. D. Bah, A. Hafiane, and R. Canals. "Deep Learning with Unsupervised Data Labeling for Weed Detection in Line Crops in UAV Images". en. In: *Remote Sensing* 10.11 (Nov. 2018). Number: 11 Publisher: Multidisciplinary Digital Publishing Institute, p. 1690. ISSN: 2072-4292. DOI: 10.3390/rs10111690. URL: https://www.mdpi.com/2072-4292/10/11/1690 (visited on 02/17/2023).

[5] R. Ramamonjison, A. Banitalebi-Dehkordi, X. Kang, X. Bai, and Y. Zhang. "SimROD: A Simple Adaptation Method for Robust Object Detection". In: *2021 IEEE/CVF International Conference on Computer Vision (ICCV)*. ISSN: 2380-7504. Oct. 2021, pp. 3550–3559. DOI: 10.1109/ICCV48922.2021.00355.

[6] N. Jaipuria, X. Zhang, R. Bhasin, M. Arafa, P. Chakravarty, S. Shrivastava, S. Manglani, and V. N. Murali. "Deflating Dataset Bias Using Synthetic Data Augmentation". In: *2020 IEEE/CVF Conference on Computer Vision and Pattern Recognition Workshops (CVPRW)*. ISSN: 2160-7516. June 2020, pp. 3344–3353. DOI: 10.1109/CVPRW50498.2020.00394.

[7] J. Valente, M. Doldersum, C. Roers, and L. Kooistra. "DETECTING *RUMEX OBTUSIFOLIUS* WEED PLANTS IN GRASSLANDS FROM UAV RGB IMAGERY USING DEEP LEARNING". English. In: *ISPRS Annals of the Photogrammetry, Remote Sensing and Spatial Information Sciences* IV-2-W5 (May 2019). Conference Name: ISPRS Geospatial Week 2019 (Volume IV-2/W5) - 10–14 June 2019, Enschede, The Netherlands Publisher: Copernicus GmbH, pp. 179–185. ISSN: 2194-9042. DOI: 10.5194/isprs-annals-IV-2-W5-179-2019. URL: https://isprs-annals.copernicus.org/articles/IV-2-W5/179/2019/isprs-annals-IV-2-W5-179-2019.html (visited on 06/01/2023).

[8] A. Etienne, A. Ahmad, V. Aggarwal, and D. Saraswat. "Deep Learning-Based Object Detection System for Identifying Weeds Using UAS Imagery". en. In: *Remote Sensing* 13.24 (Jan. 2021). Number: 24 Publisher: Multidisciplinary Digital Publishing Institute, p. 5182. ISSN: 2072-4292. DOI: 10.3390/rs13245182. URL: https://www.mdpi.com/2072-4292/13/24/5182 (visited on 06/09/2023).

[9] A. Wang, T. Peng, H. Cao, Y. Xu, X. Wei, and B. Cui. "TIA-YOLOv5: An improved YOLOv5 network for real-time detection of crop and weed in the field". In: *Frontiers in Plant Science* 13 (Dec. 2022), p. 1091655. ISSN: 1664-462X. DOI: 10.3389/fpls.2022.1091655. URL: https://www.ncbi.nlm.nih.gov/pmc/articles/PMC9815699/ (visited on 01/19/2023).

[10] A. Milioto, P. Lottes, and C. Stachniss. "Real-Time Semantic Segmentation of Crop and Weed for Precision Agriculture Robots Leveraging Background Knowledge in CNNs". In: *2018 IEEE International Conference on Robotics and Automation (ICRA)*. ISSN: 2577-087X. May 2018, pp. 2229–2235. DOI: 10.1109/ICRA.2018.8460962.

[11] S. K. Valicharla. "Weed Recognition in Agriculture: A Mask R-CNN Approach". In: *Graduate Theses, Dissertations, and Problem Reports* (Jan. 2021). DOI: https://doi.org/10.33915/etd.8102. URL: https://researchrepository.wvu.edu/etd/8102.

[12] Y. Mu, R. Feng, R. Ni, J. Li, T. Luo, T. Liu, X. Li, H. Gong, Y. Guo, Y. Sun, Y. Bao, S. Li, Y. Wang, and T. Hu. "A Faster R-CNN-Based Model for the Identification of Weed Seedling". en. In: *Agronomy* 12.11 (Nov. 2022). Number: 11 Publisher: Multidisciplinary Digital Publishing Institute, p. 2867. ISSN: 2073-4395. DOI: 10.3390/agronomy12112867. URL: https://www.mdpi.com/2073-4395/12/11/2867 (visited on 06/08/2023).

[13] J. Gao, W. Liao, D. Nuyttens, P. Lootens, J. Vangeyte, A. Pižurica, Y. He, and J. G. Pieters. "Fusion of pixel and object-based features for weed mapping using unmanned aerial vehicle imagery". en. In: *International Journal of Applied Earth Observation and Geoinformation* 67 (May 2018), pp. 43–53. ISSN: 1569-8432. DOI: 10.1016/j.jag.2017.12.012. URL: https://www.sciencedirect.com/science/article/pii/S0303243417303252 (visited on 06/09/2023).

[14] E.-S. M. El-Kenawy, N. Khodadadi, S. Mirjalili, T. Makarovskikh, M. Abotaleb, F. K. Karim, H. K. Alkahtani, A. A. Abdelhamid, M. M. Eid, T. Horiuchi, A. Ibrahim, and D. S. Khafaga. "Metaheuristic Optimization for Improving Weed Detection in Wheat Images Captured by Drones". en. In: *Mathematics* 10.23 (Jan. 2022). Number: 23 Publisher: Multidisciplinary Digital Publishing Institute, p. 4421. ISSN: 2227-7390. DOI: 10.3390/math10234421. URL: https://www.mdpi.com/2227-7390/10/23/4421 (visited on 06/09/2023).

[15] C. Hu, J. A. Thomasson, and M. V. Bagavathiannan. "A powerful image synthesis and semi-supervised learning pipeline for site-specific weed detection". en. In: *Computers and Electronics in Agriculture* 190 (Nov. 2021), p. 106423. ISSN: 01681699. DOI: 10.1016/j.compag.2021.106423. URL: https://linkinghub.elsevier.com/retrieve/pii/S0168169921004403 (visited on 01/19/2023).

[16] S. Xie, C. Hu, M. Bagavathiannan, and D. Song. "Toward Robotic Weed Control: Detection of Nutsedge Weed in Bermudagrass Turf Using Inaccurate and Insufficient Training Data". English. In: *IEEE robotics and automation letters* 6.4 (2021). Place: Piscataway

Publisher: IEEE, pp. 7365–7372. ISSN: 2377-3766. DOI: 10.1109/LRA.2021.3098012. URL: https://go.exlibris.link/01qqrgGz (visited on 01/19/2023).

[17] B. B. Sapkota, S. Popescu, N. Rajan, R. G. Leon, C. Reberg-Horton, S. Mirsky, and M. V. Bagavathiannan. "Use of synthetic images for training a deep learning model for weed detection and biomass estimation in cotton". en. In: *Scientific Reports* 12.1 (Nov. 2022). Number: 1 Publisher: Nature Publishing Group, p. 19580. ISSN: 2045-2322. DOI: 10.1038/s41598-022-23399-z. URL: https://www.nature.com/articles/s41598-022-23399-z (visited on 03/14/2023).

[18] J. Su, D. Yi, M. Coombes, C. Liu, X. Zhai, K. McDonald-Maier, and W.-H. Chen. "Spectral analysis and mapping of blackgrass weed by leveraging machine learning and UAV multispectral imagery". en. In: *Computers and Electronics in Agriculture* 192 (Jan. 2022), p. 106621. ISSN: 0168-1699. DOI: 10.1016/j.compag.2021.106621. URL: https://www.sciencedirect.com/science/article/pii/S0168169921006384 (visited on 05/29/2023).

[19] J. P. Lambert, D. Z. Childs, and R. P. Freckleton. "Testing the ability of unmanned aerial systems and machine learning to map weeds at subfield scales: a test with the weed Alopecurus myosuroides (Huds)". en. In: *Pest Management Science* 75.8 (2019). _eprint: https://onlinelibrary.wiley.com/doi/pdf/10.1002/ps.5444 paper:cite_key, pp. 2283–2294. ISSN: 1526-4998. DOI: 10.1002/ps.5444. URL: https://onlinelibrary.wiley.com/doi/abs/10.1002/ps.5444 (visited on 06/20/2023).

[20] G. A. Mini, D. Oliva Sales, and M. Luppe. "Weed segmentation in sugarcane crops using Mask R-CNN through aerial images". In: *2020 International Conference on Computational Science and Computational Intelligence (CSCI)*. Dec. 2020, pp. 485–491. DOI: 10.1109/CSCI51800.2020.00088.